2017

Light Diffraction Patterns for Telescope Application

Daniel Yates
Pacific University

Light Diffraction Patterns for Telescope Application

Abstract
Modern optical telescopes are giving us unprecedented imaging of the Universe in order to probe into the nature of dark matter and dark energy. Large optical telescopes require complex optical systems—often involving multiple lenses and mirrors. Light diffraction patterns on the focal planes influence imaging resolution, so a good understanding of diffraction is required to ensure high precision imaging. This project examines elements of diffraction—such as the Huygens-Fresnel Principle and the point spread function—to understand how they influence telescope optics. In addition, this project compares different diffraction theories, including Kirchhoff, Fraunhofer, and Fresnel diffraction, in order to determine similarities and differences between the diffraction theories.

Document Type
Thesis

Department
Mathematics

Subject Categories
Mathematics

Comments
Honorable Mention, 2017 CommonKnowledge Senior Project Writing Award

Light Diffraction Patterns for Telescope Application

Daniel Yates

Department of Mathematics
Pacific University

This capstone is submitted for the degree of
Bachelor of Science in Mathematics

College of Arts and Sciences August 2017

Abstract

Modern optical telescopes are giving us unprecedented imaging of the Universe in order to probe into the nature of dark matter and dark energy. Large optical telescopes require complex optical systems—often involving multiple lenses and mirrors. Light diffraction patterns on the focal planes influence imaging resolution, so a good understanding of diffraction is required to ensure high precision imaging. This project examines elements of diffraction—such as the Huygens-Fresnel Principle and the point spread function—to understand how they influence telescope optics. In addition, this project compares different diffraction theories, including Kirchhoff, Fraunhofer, and Fresnel diffraction, in order to determine similarities and differences between the diffraction theories.

Chapter 1

Optical Telescopes

1.1 Introduction

Telescopes have greatly transformed our knowledge of the Universe. From the first telescopes that were used to view the moon to the current large telescopes reaching into the far corners of the Universe, they continue to increase the current knowledge of the Universe and physics.

Light diffraction patterns are some of the hardest problems in optics to solve, with many relying on various assumption and simplifications in order to make the problems solvable [6]. This project is focused both on understanding the mathematical derivations and techniques that are used in order to achieve the diffraction formulas that are commonly used to solve diffraction problems, and applying them to telescope.

1.2 Early Optical Telescopes

The famous astronomer Galileo Galilei is credited with the first functional astronomical telescope design. In July of 1609, just months after the Dutch lens maker Hans Lippershey had used two lenses together to magnify a far-off church tower, Galileo assembled two lenses–one concave and one convex–into a functional telescope system, known today as a Galilean Telescope. This design consisted of a convex mirror nearest the object–known as the objective lens–and a concave lens as the eyepiece nearest the observer [4].

Just two years after Galileo first created his telescope, Johannes Kepler invented a similar astronomical telescope. The Keplerian Telescope used two convex mirrors rather than the concave/convex combination used in the Galilean Telescope. By using a convex lens in the eyepiece, the Kepler Telescope is capable of a slightly wider field of view than that of the

Galilean Telescope; however, the lack of the concave eyepiece creates an inverted image, unlike that of the Galilean Telescope [4].

1.3 Reflecting Telescopes

Although the Galilean and Keplerian Telescopes are simple and useful telescopes, they are not without problems. The main difficulty in using a lens-based telescope are the chromatic aberrations–fringing of colors on an image–associated with it. These aberrations arise from different wavelengths of light traveling through the glass lenses, which have a slightly different index of refraction than air. To counteract these aberrations, Dutch astronomer Christiaan Huygens proposed the idea of of using lenses with very small curvatures in order to curb the aberrations as much as possible. Unfortunately, decreasing the curvature increases the focal length of the lens, leading to telescopes with tube lengths of many meters [4].

In order to both correct for chromatic aberrations and prevent impractical tube lengths, James Gregory put forward the idea of using reflecting telescopes rather than refracting telescopes. In 1664, Gregory proposed the Gregorian Telescope design, which uses conic section mirrors in place of the glass lenses used in Galilean and Keplerian Telescopes. Due to difficulties in the manufacturing of the elliptical concave mirrors needed for the telescope, Gregory never actually built one of these models [4].

Sir Isaac Newton, on the other hand, produced a working reflective telescope in January of 1670. Newton used a parabolic mirror in place of the concave mirror to allow easier manufacturing of the telescope and to prevent aberrations from appearing, as the parabolic mirror ensures that all parallel incoming light rays are focused on the focal point of the mirror [4]. Examples of Galilean, Keplerian, and Newtonian telescope designs are shown in Figure 1.1. Variations on telescopes such as these are currently being used to discover more about the nature of dark energy and dark matter, as well as mapping both galactic and solar structure.

1.4 Modern Optical Telescopes

Current optical telescopes are much more powerful than the simple telescopes used by Galileo and Newton centuries ago. Survey telescopes currently in use have primary mirrors with diameters on the order of 8 meters or larger. These massive telescopes provide great benefits over the smaller, earlier telescope designs used in the past. Large telescopes, such as the Large Synoptic Survey Telescope, have large fields of view and high resolution that allows scientists to uncover more information about the universe. For instance, the Large Synoptic

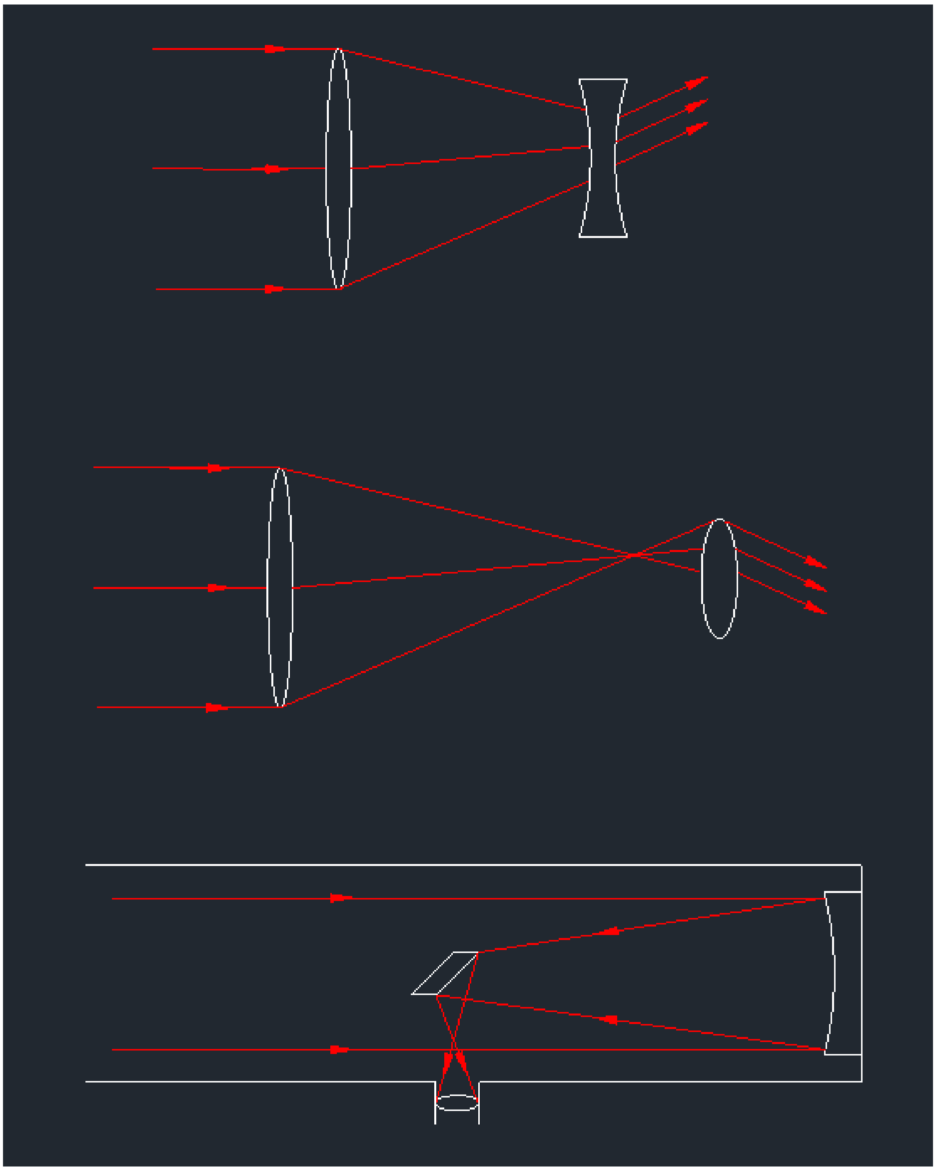

Fig. 1.1 Examples of Galilean (top), Keplerian (middle), and Newtonian (bottom) telescopes and how light transits through the telescopes to the aperture.

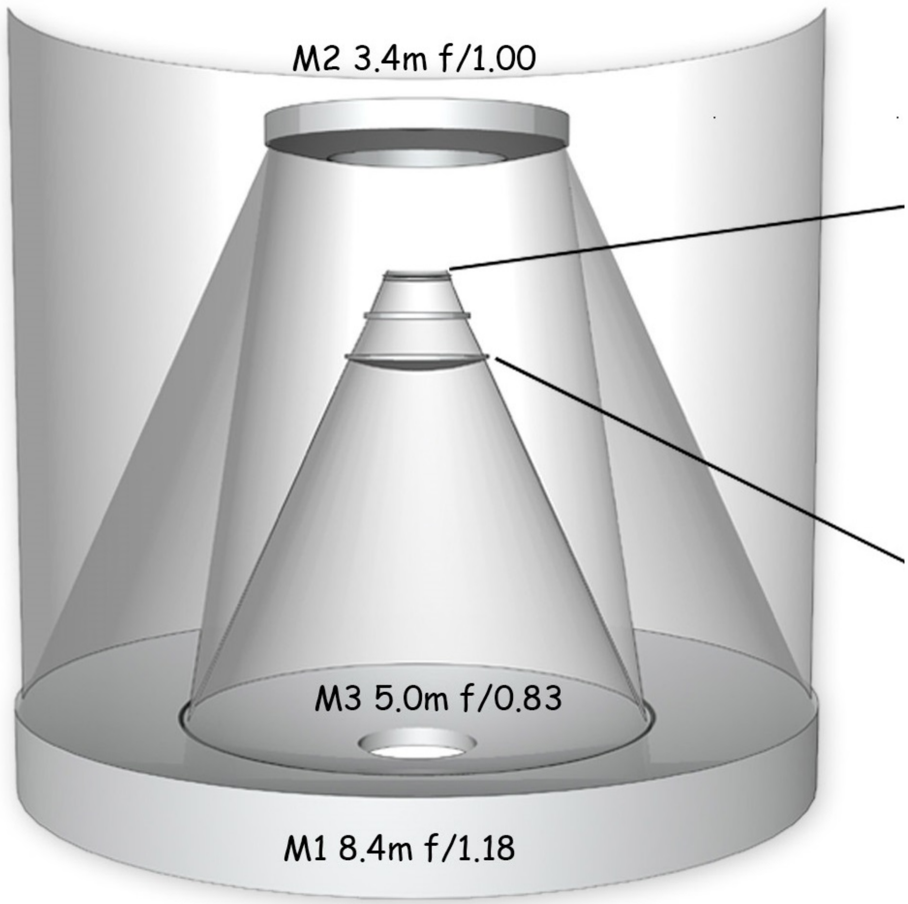

Fig. 1.2 Optical design of the Large Synoptic Survey Telescope, showing the light cones for each mirror as light transits through the mirror system and into the camera. The three mirrors (M1, M2, M3) provide the mirror diameter and focal length/aperture ratio [5].

Survey Telescope (figure 1.2), currently being built for a ten-year survey mission in Chile, has a 3.5 degree field of view and a resolution of less than 1 arcsecond [5].

1.5 Properties of Light

Light acts as an electromagnetic wave that propagates at the speed of light ($c = 3 \times 10^8 m/s$) through the electromagnetic spectrum. Light that is spherically emitted from a source will oscillate through space as e^{ikr}, where the wavenumber k is defined as $2\pi/\lambda$, with λ denoting the wavelength of light, and r denotes the distance from the emission source. Additionally, the amplitude decays as $1/r$, so that the total amplitude of light at a distance r from the source is given as $U(r) = Ae^{ikr}/r$, where A is the initial amplitude of the light at the source [6].

Because light acts as a wave, it experiences properties of waves–one of which is interference between waves. An example of such interference is shown in Figure 1.3. When the peaks and valleys of the two waves line up, the waves add in amplitude in what is known as constructive interference. Similarly, when the peak of one wave lines up with the valley of another, the waves undergo destructive interference and sum to zero net amplitude.

Since light waves undergo interference, there are a number of peculiar phenomena that arise from the self-interference of light. One interesting result is seen in a single-slit diffraction experiment. An example of a single-slit diffraction experiment is shown in Figure 1.4. As light waves move through the slit, they spread out and begin to interfere with each other. The pattern displayed on a screen, as shown in Figure 1.4, depends on the offset angle from directly normal to the slit. With a slit of width d, the locations of maxima–which correspond to constructive interference–occur at angles α from the center of the screen given by the equation $dsin(\alpha) = n\lambda$, where n is an integer [3].

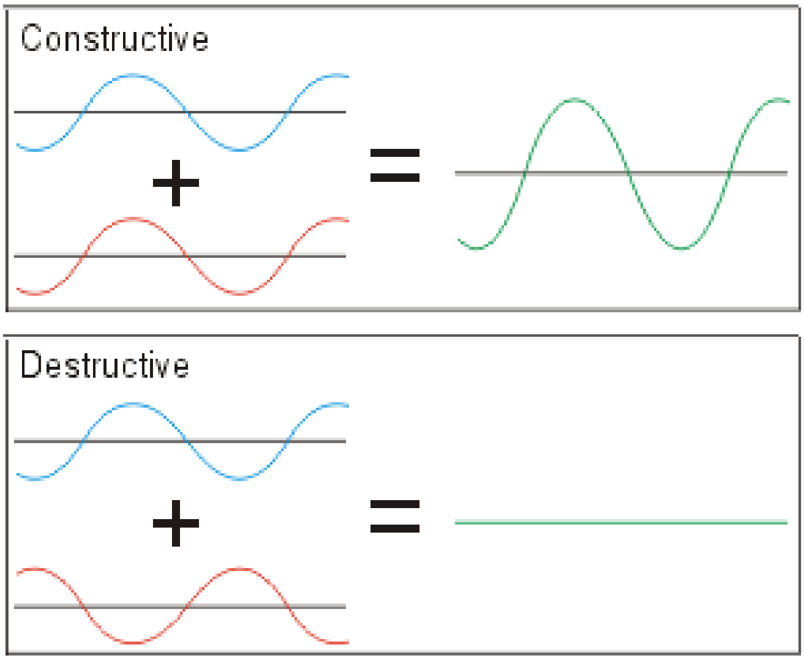

Fig. 1.3 Examples of constructive and destructive interference between two waves of light [7].

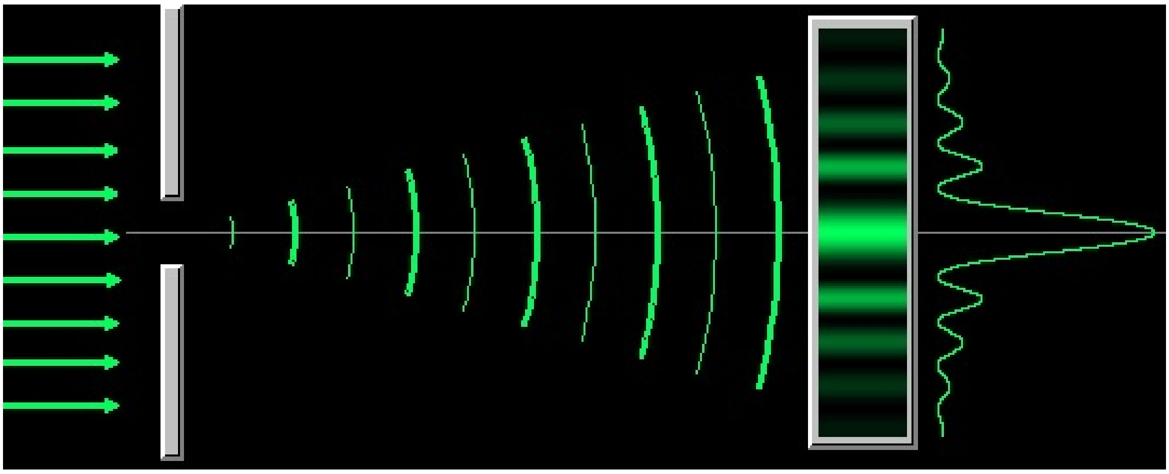

Fig. 1.4 Example of single slit experiment, with intensity pattern shown on the right [1].

Chapter 2

Diffraction Patterns on Telescope Apertures

The following derivations closely follow the treatment in [6], pgs 412-426.

2.1 Huygens-Fresnel Principle

The first step in understanding diffraction patterns of light through an aperture is the Huygens-Fresnel Principle. As light emitted from a point source passes through a slit, the wavefront of light does not continue on completely unimpeded through the slit; rather, the light begins to spread out after passing through the slit. An example of this phenomenon can be seen in Figure 2.1.

Christiaan Huygens proposed that, in order to evaluate the distorted wavefront, one can model the wavefront as a collection of secondary point sources. These secondary wavelets originate on the original wavefront, and the resulting wavefront after the light passes through the slit is the envelope of the interference between all of the secondary light sources. This theory is often referred to as the Huygens-Fresnel Principle.

By modeling light diffraction using the Huygens-Fresnel Principle, the amplitude of light at a point due to a source of light can be evaluated by examining the contributions from the secondary wavelets. One can determine the amplitude of light at point P due to light being emitted from point P_0 by examining the small contributions due to a given wavefront, as shown in Figure 2.2.

The small contribution at the point P due to a point on the wavefront is given by

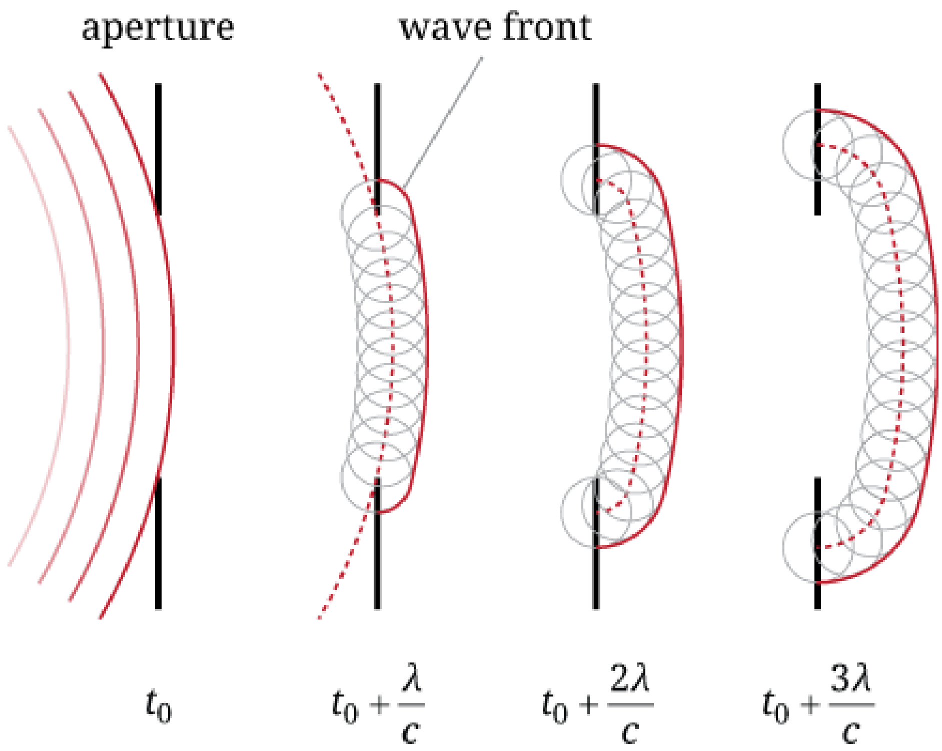

Fig. 2.1 Example of spreading of wavefront as it propagates through a slit [8].

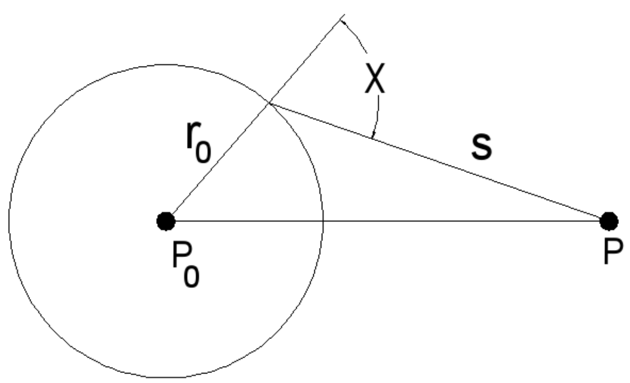

Fig. 2.2 Example of light being emitted from point P_0 to be evaluated at point P.

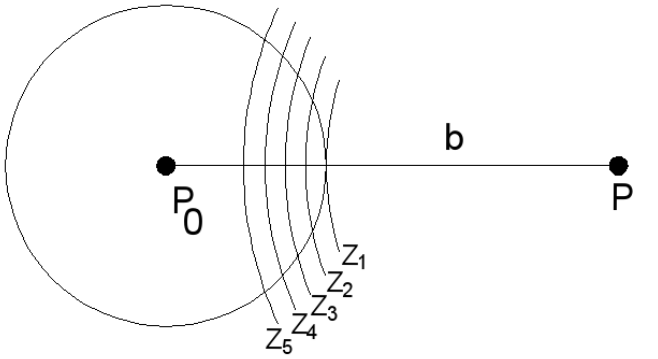

Fig. 2.3 Example of zonal construction outward from point P.

$$dU(P) = K(\chi)\frac{Ae^{ikr_0}}{r_0}\frac{e^{iks}}{s}dS \tag{2.1}$$

where the $\frac{Ae^{ikr_0}}{r_0}$ term gives the light amplitude at the point on the wavefront, $\frac{e^{iks}}{s}$ denotes the light amplitude between the wavefront and the point P, and $K(\chi)$ is the inclination factor. The inclination factor is used to describe the amount of light that was initially emitted from P_0 that will contribute to point P, as not all light on the wavefront will be redirected towards point P. The angle χ denotes the angle between normal to the wavefront and the direction towards point P and is often called the angle of diffraction. The expectation for the inclination factor is that the function is maximized at $\chi = 0$ and zero at $\chi = \pm\pi/2$.

The total amplitude of light $U(P)$ at point P is given by the integral along the wavefront S:

$$U(P) = \frac{Ae^{ikr_0}}{r_0}\iint_S K(\chi)\frac{e^{iks}}{s}dS \tag{2.2}$$

To evaluate the integral, Fresnel proposed using a method known as zonal construction. With this method, zones are constructed outward from the point P at half-wavelength radii, with the first zone Z_1 being constructed at a radius b, where $b + r_0$ is the distance between P_0 and P (Figure 2.3). By creating these zones, the inclination factor can be approximated as constant along a given zone.

By using n zones in the zonal construction, the light amplitude $U(P)$ can be approximated as

$$U(P) = i\lambda(K_1 \pm K_n)\frac{Ae^{ik(r_o+b)}}{r_0+b} \tag{2.3}$$

Due to the previous assumption that $K(0) = 0$, the K_n term goes to zero, and thus

$$U(P) = i\lambda K_1 \frac{Ae^{ik(r_0+b)}}{r_0+b} = \frac{1}{2}U_1(P) \tag{2.4}$$

Because there does not yet exist a slit, the light amplitude given by equation 2.4 must equal that of spherically emitted light. This gives an approximation for the inclination factor at $\chi = 0$ as $K(0) = -i/\lambda$.

2.2 Kirchhoff Diffraction Integral

While the Huygens-Fresnel Principle can be used to approximate the light amplitude due to diffraction through a slit, Gustav Kirchhoff proposed that in actuality, the Huygens-Fresnel Principle was merely an approximation of a more comprehensive integral. This integral would become known as Kirchhoff's Integral Theorem or the Integral Theorem of Helmholtz and Kirchhoff.

The derivation of Kirchhoff's Integral Theorem begins by examining the spatial component of a monochromatic (single-wavelength) light wave given by

$$V(x,y,z,t) = U(x,y,z) \cdot e^{-i\omega t} \tag{2.5}$$

where $U(x,y,z)$ denotes the spatial component and $\omega = 2\pi c/\lambda$ Because U is a wave, it satisfies the Helmholtz equation (steady-state wave equation):

$$(\Delta + k^2)U = 0. \tag{2.6}$$

Furthermore, let there exist a function U' that also satisfies the Helmholtz equation, and let both U and U' both posses continuous first and second order partial derivatives.

The amplitude of light at a point P can be evaluated by examining the contributions from U and U' within a volume V that encloses P by a closed surface S, as seen in Figure 2.4. By defining $\frac{\partial}{\partial n}$ as differentiation along the inward normal, then by Green's Theorem:

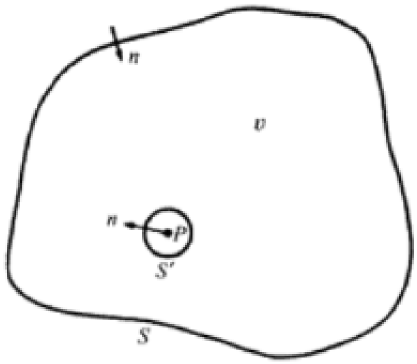

Fig. 2.4 Example of arbitrary surfaces S and S' enclosing point P [6].

$$\iiint_V \left(U\Delta U' - U'\Delta U\right) dV = -\iint_S \left(U\frac{\partial U'}{\partial n} - U'\frac{\partial U}{\partial n}\right) dS = 0. \tag{2.7}$$

Due to the fact that U and U' satisfy the Helmholtz equation, the integrand of the volume integral is zero, giving the total equation equal to zero as well.

Let the function $U' = \frac{e^{iks}}{s}$, where S denotes the distance from P to a point within the volume. Unfortunately, with this assumption of U', there now exists a singularity at $s = 0$. To handle this, one can encompass the point P by a small surface S' of radius ε, as shown in Figure 2.4. Then the surface integral in equation 2.7 can be expressed as

$$\left[\iint_S + \iint_{S'}\right]\left\{U\frac{\partial U'}{\partial n} - U'\frac{\partial U}{\partial n}\right\} dS = 0 \tag{2.8}$$

or

$$\iint_S \left[U\frac{\partial U'}{\partial n} - U'\frac{\partial U}{\partial n}\right] dS = -\iint_{S'} \left[U\frac{\partial U'}{\partial n} - U'\frac{\partial U}{\partial n}\right] dS. \tag{2.9}$$

Due to the fact that the surface S' exists at a distance $s = \varepsilon$ from point P, the substitution can be made of $S' = \varepsilon^2\Omega$, where Ω denotes the solid angle of S'.

When substituting in $s = \varepsilon$ into equation 2.8 and taking the appropriate derivatives, the integral on the left hand side (LHS) is now independent of ε on the right hand side (RHS):

$$\iint_S \left(U\frac{\partial U'}{\partial n} - U'\frac{\partial U}{\partial n}\right)dS = -\iint_\Omega \left(U\frac{e^{ik\varepsilon}}{\varepsilon}\left(ik - \frac{1}{\varepsilon}\right) - \frac{e^{ik\varepsilon}}{\varepsilon}\frac{\partial U}{\partial s}\right)\varepsilon^2 d\Omega \tag{2.10}$$

and the RHS integral can be evaluated in the limit as $\varepsilon \to 0$ [6].

With the limiting case of $\varepsilon \to 0$, the first and third terms on the RHS approach zero, and the second term yields $4\pi U$. Thus, the LHS integral is precisely that of Kirchhoff's Integral Theorem:

$$U(P) = \frac{1}{4\pi}\iint_S \left[U\frac{\partial}{\partial n}\left(\frac{e^{iks}}{s}\right) - \frac{e^{iks}}{s}\frac{\partial U}{\partial n}\right]dS \tag{2.11}$$

where $k = 2\pi/\lambda$, s is the distance from the point P to the contribution point within S, and $\frac{\partial}{\partial n}$ is differentiation along the inward normal of S.

2.3 Kirchhoff's Diffraction Theory

With the Kirchhoff Integral Theorem for diffraction (equation 2.11), it is possible to now analyze the light amplitude pattern at a point P after light has traveled through a slit from the source P_0. The next step to understanding this diffraction theorem is to apply it to a simple slit case.

Consider Figure 2.5, where again light emits from point P_0 and is going to be evaluated at point P. However, there now exists a slit and block that allow only some of the light from P_0 to P. By defining the slit as A, the block on either side of the slit as B, and a surface C that creates a closed surface out of A, B, and C. Then the Kirchhoff Diffraction Integral can be expressed as

$$U(P) = \frac{1}{4\pi}\left[\iint_A + \iint_B + \iint_C\right]\left\{U\frac{\partial}{\partial n}\left(\frac{e^{iks}}{s}\right) - \frac{e^{iks}}{s}\frac{\partial U}{\partial n}\right\}dS. \tag{2.12}$$

With the example in Figure 2.5, some simplifying assumptions can be made: the first being that, along the slit A, the light will be essentially unchanged except immediately near the boundaries of A and B. Additionally, along the surface B, the light will not exist due to being blocked by the slit block. Finally, for the boundary C, since C is arbitrary, it can be

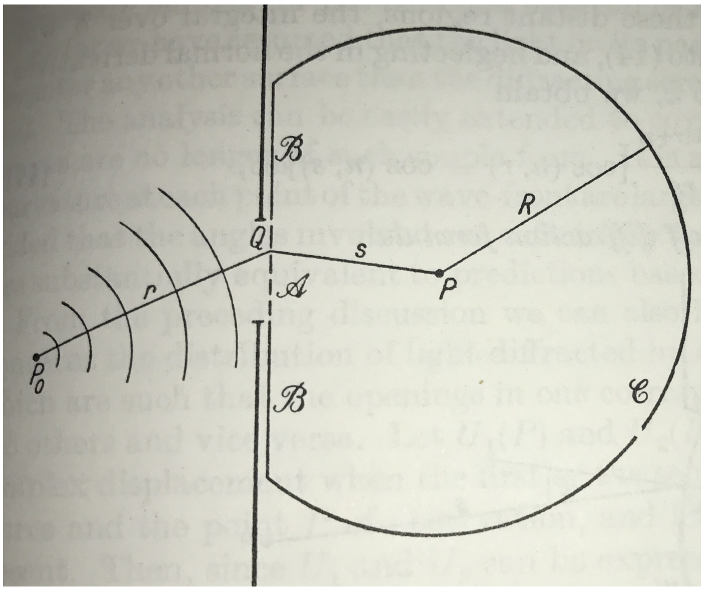

Fig. 2.5 Example of slight transversing a slit after being emitted from point P [6].

extended to infinity. Because the light amplitude decays as $1/r$, at infinity the amplitude of the light will be zero, and thus contributions from the integral over C will be zero as well.

Furthermore, working under the assumption that both P and P_0 are far from the slit compared to the slit length, then edge effects at the A/B intersections can be neglected, the integral can be further simplified into

$$U(P) = -\frac{i}{2\lambda}\frac{U_0 e^{ikr_0}}{r_0}\iint_A \frac{e^{iks}}{s}(1+cos\chi)dS \tag{2.13}$$

where U_0 is the initial amplitude of light at P_0, $k = 2\pi/\lambda$, r_0 is the distance from P_0 to a point on the slit, and s is the distance from a point on the slit to P. In-depth arguments for the simplifications from equations 2.12 to 2.13 can be found in.

Equation 2.13 gives a good approximation for the inclination factor $K(\chi)$ that was used in section 2.1. By comparing equation 2.13 to equation 2.2, in order for continuity between the two, the inclination factor can be approximated as

$$K(\chi) = -\frac{i}{2\lambda}(1+cos\chi) \tag{2.14}$$

which, for the $\chi = 0$ case, does in fact agree with the approximation that $K(0) = -i/\lambda$; however, it does not agree with the assumption that $K(\pi/2) = 0$ [6].

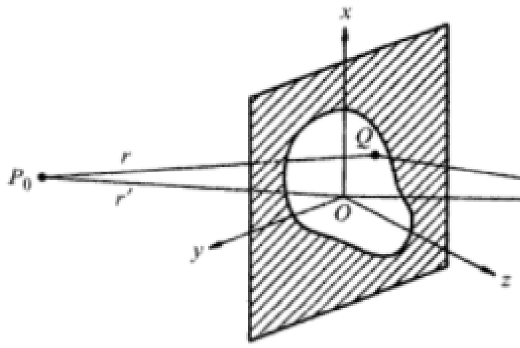

Fig. 2.6 Example of light traveling through a 2-dimensional aperture [6].

2.4 Fraunhofer and Fresnel Diffraction Criteria

Using equation 2.13, both the Fraunhofer and Fresnel diffraction criteria can be derived using a few more approximations. Figure 2.6 shows again light being emitted from P_0 to P, but traveling through a 2-dimensional aperture instead of a 1-dimensional slit.

Firstly, the distance from P_0 to the aperture r is not a constant, so it must be placed back in the integral. Under the assumption again that both P_0 and P are far from the slit, then the $1+cos\chi$ term can be replaced by a term $2cos\delta$, where δ denotes the angle that a line between P_0 and P makes with the aperture surface. So, Kirchoff's Integral Theorem can be approximated as

$$U(P) = -\frac{U_0 icos\delta}{\lambda} \iint_A \frac{e^{ik(r+s)}}{rs} dS \tag{2.15}$$

Due to the fact that r and s are large and will not change appreciably over the aperture, they can be replaced with r' and s', respectively, and pulled out of the integral. As can be seen in figure 2.6, the variables r' and s' denote the distances from P_0 to the coordinate origin and from said origin to P, respectively. Thus, the integral can be simplified further to

$$U(P) = -\frac{U_0 icos\delta}{\lambda r' s'} \iint_A e^{ik(r+s)} dS \tag{2.16}$$

where now solving for the light amplitude at P consists of evaluating an exponential.

While still not trivial, one more approximation can be made that ends up defining different diffraction criteria. Let the arbitrary point Q on the aperture (Figure 2.6) be located at the point $(\xi,\eta,0)$. Then with the points P_0 and P located at (x_0,y_0,z_0) and (x,y,z), respectively, the four distances r, r', s, s' can be defined as

$$\begin{aligned} r^2 &= (x_0-\xi)^2+(y_0-\eta)^2+z_0^2 \\ s^2 &= (x-\xi)^2+(y-\eta)^2+z^2 \end{aligned} \tag{2.17}$$

$$\begin{aligned} (r')^2 &= x_0^2+y_0^2+z_0^2 \\ (s')^2 &= x^2+y^2+z^2. \end{aligned} \tag{2.18}$$

Through a combination of equations 2.17 and 2.18, the r term may be expanded as a power series in r' about $(\xi,\eta)=(0,0)$:

$$r \sim r' - \frac{x_0\xi+y_0\eta}{r'} + \frac{\xi^2+\eta^2}{2r'} - \frac{(x_0\xi+y_0\eta)^2}{2(r')^3} + \ldots \tag{2.19}$$

with an analogous power series expansion of s in terms of s', x, and y.

These power series expansions are crucial to understanding light diffraction through an aperture. In fact, the power series themselves define two different diffraction criteria: Fraunhofer and Fresnel diffraction. Fraunhofer diffraction arises when the second order and higher terms in ξ and η may be neglected, as their contributions are insignificant compared to the linear terms in the power series. If, however, the quadratic terms of ξ and η must be considered, then one speaks of Fresnel diffraction instead.

Chapter 3

Diffraction Applications

3.1 Circular Telescope Aperture

The expression for light amplitude in equation 2.16 can be used to evaluate the diffraction pattern on a circular aperture–like telescopes, for instance. For light being imaged on telescope, the assumption of Fraunhofer diffraction can be made, as the sources of light are very far away compared to the aperture diameter. By casting the locations of Q, a given point in the aperture and P in polar coordinates as $(\xi, \eta) = (\rho, \theta)$ and $P = (w, \psi)$, respectively, then the expression for the light amplitude becomes

$$U(P) = C\int_0^{2\pi}\int_0^a e^{-ik\rho w cos(\theta-\psi)}\rho d\rho d\theta \tag{3.1}$$

where a is the aperture radius and C is the complex constant from equation 2.16 involving the wavelength of light and locations of the source and image point [6].

Evaluation of the double integral in (3.1) involves the Bessel functions, which are a set of functions solving the following differential equation for different cases of n:

$$x^2\frac{d^2y}{dx^2} + x\frac{dy}{dx} + y(x^2 - n) = 0. \tag{3.2}$$

By using the two Bessel function recurrence relations of

$$J_n(x) = \frac{i^{-n}}{2\pi}\int_0^{2\pi} e^{ixcos\alpha}e^{in\alpha}d\alpha \tag{3.3}$$

and

$$x^{n+1}J_n(x) = \frac{d}{dx}[x^{n+1}J_{n+1}(x)], \tag{3.4}$$

then the light amplitude at point P is given as

$$U(P) = \pi a^2 C \frac{2J_1(kaw)}{kaw}. \tag{3.5}$$

Thus, the characterizing function of the light amplitude is given as a 1^{st} order Bessel function over its argument [6].

The intensity of the light–what one physically thinks of and can detect–is given as the square of the amplitude of light. Thus, the intensity of light at P is

$$I(P) = |U(P)|^2 = \left(\frac{2J_1(kaw)}{kaw}\right)^2 I_0 \tag{3.6}$$

where I_0 is the light intensity at the source P_0. A plot of the characterizing function $\frac{J_1(x)^2}{x^2}$ is given in Figure 3.1.

The 1-dimensional representation of the intensity pattern in Figure 3.1 can be translated into a 2-dimensional representation through rotation about the y-axis of the figure. By taking a top-down view, one witnesses the intensity pattern shown in Figure 3.2. A large peak of high intensity exists at the center of the aperture, and then alternating rings of dark and light correspond to the maxima and minima in the graph in Figure 3.1. Indeed, the pattern shown in Figure 3.2 is what is physically observed with diffraction through a circular aperture. The pattern shown in Figure 3.2 is known as the Airy disk [6].

3.2 Aperture Block

A further application of the circular aperture diffraction pattern is to describe the pattern formed when an aperture block is present. For example, in a 2-mirror telescope like in Figure 3.3, the secondary mirror blocks some of the incoming light that will influence the diffraction pattern.

In the case of an aperture stop of radius ca, where $c < 1$, the integral in equation 3.1 is evaluated from ca to a rather than from 0 to a. The result of this change in integration limits gives a difference in first-order Bessel functions:

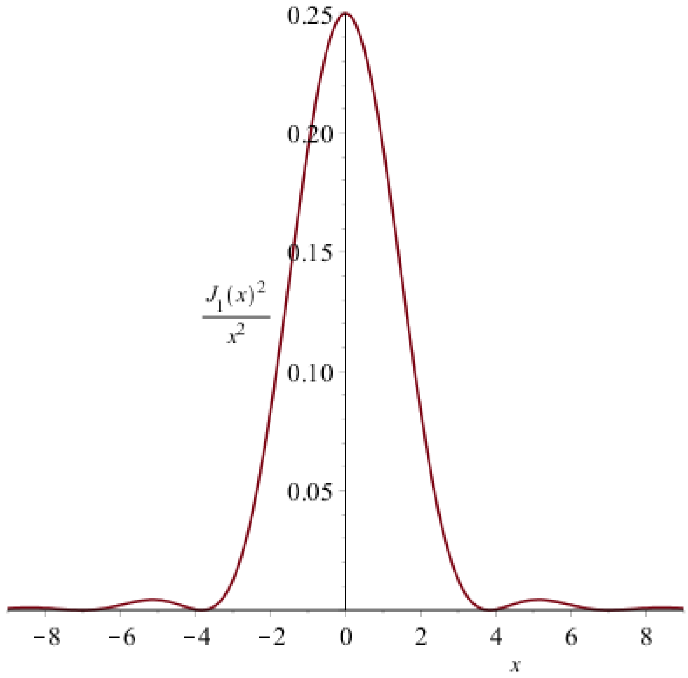

Fig. 3.1 Plot of characterizing function of light intensity on circular telescope aperture.

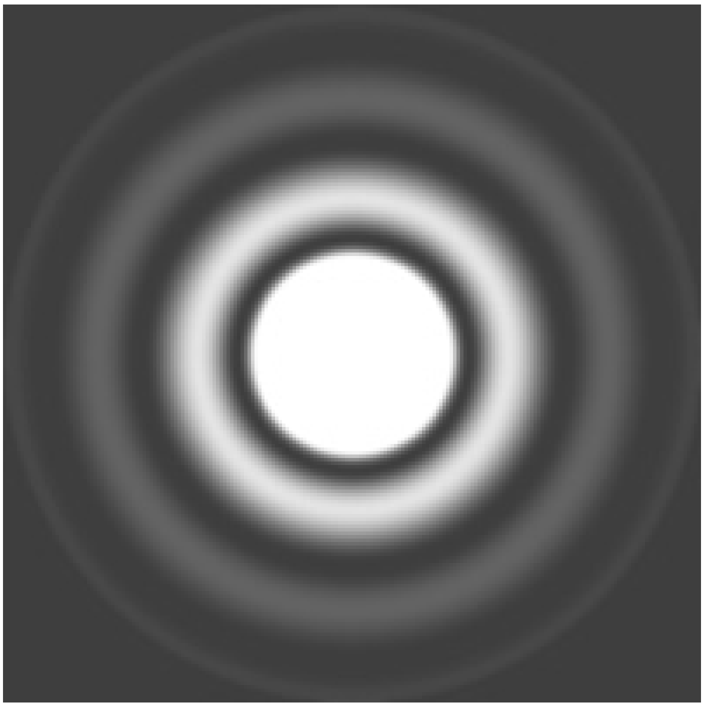

Fig. 3.2 Example of light intensity pattern due to diffraction through a circular aperture, commonly known as the Airy disk [2].

Fig. 3.3 Example of 2-mirror telescope.

$$I(P) = \frac{1}{(1-c^2)^2}\left[\left(\frac{2J_1(kaw)}{kaw}\right) - c^2\left(\frac{2J_1(ckaw)}{ckaw}\right)\right]^2 I_0. \tag{3.7}$$

The extra term in equation 3.7 is due to the radius integral starting at a nonzero value [6].

The effects of differing aperture block sizes can be seen in Figure 3.4. Compared to Figure 3.1, the maximum value of the function at the center is decreased when the aperture block is implemented. Increasing the ratio of the aperture block to the total aperture size causes a decrease in the maximum value of the peak.

Interestingly enough, while increasing size of the block decreases the peak value, it also causes a narrowing the peak width. So, for telescopes that are in search of faint stars only, then the ideal setup seems to be one without a block. The introduction of a block would increase resolving power of the telescope due to the narrowing of widths of the principle peaks in the image formed. This increased resolving power comes at the cost of losing intensity overall for the image formed; longer exposure times are thus needed to obtain usable images.

3.3 Conclusions

Diffraction problems, being some of the most complex problems to solve in optics, require a thorough understanding of many concepts in order to derive the equations needed to evaluate light patterns. Understanding the derivation of Kirchhoff's Integral Theorem from the Huygens-Fresnel Principle is crucial to being able to get insight into and mathematically describe the diffraction patterns through apertures. Light diffraction through a circular aperture gives an intensity pattern known as the Airy disk, with a bright peak at the center of

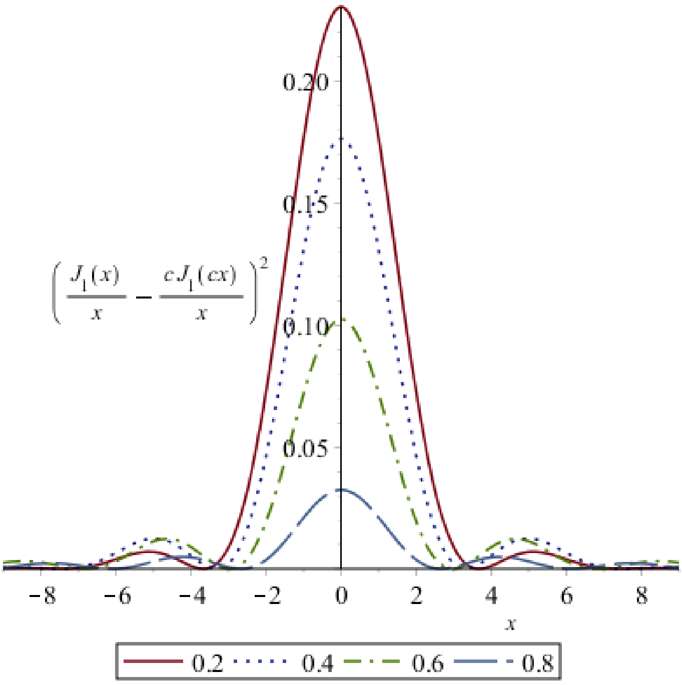

Fig. 3.4 Plot of intensity of light with aperture blocks of various sizes.

the image plane and subsequent rings of bright and dark moving outwards. The introduction of an aperture block decreases the intensity of peaks, but also increases resolving power of the telescope. While not exact close-form solutions to diffraction problems, the derivations understood in paper make initial analysis of these problems more easily understood.

Acknowledgements

I would like to thank Dr. Guenther for mentoring me on this project. I would also like to thank the Pacific University Department of Mathematics for support over my college career.

Bibliography

[1] Marianne Breinig. *Single Slit Diffraction*, n.d. URL http://labman.phys.utk.edu/phys222core/modules/m9/images/diffra13.gif.

[2] Cambridge in Colour. *Lens Diffraction and Photography*, n.d. URL http://www.cambridgeincolour.com/tutorials/diffraction-photography.htm.

[3] Bill Casselman. *Single Slit Diffraction Pattern of Light*, 2003. URL http://www.math.ubc.ca/~cass/courses/m309-03a/m309-projects/krzak/.

[4] Jingquan Cheng. *The Principles of Astronomical Telescope Design*. Springer Science & Business Media, 2010.

[5] LSST Corporation. *The Large Synoptic Survey Telescope*, 2016. URL www.lsst.org.

[6] Max Born & Emil Wolf. *Principles of Optics*. Cambridge University Press, 2002.

[7] ThingLink. *Constructive Interference and Destructive Interference*, 2015. URL http://s1.thingpic.com/images/DF/QjQNCQ2eMfcLWJRa3k4gC6uB.png.

[8] Marcus Winter. *Scalar Diffraction- Huygens, Fresnel, Fraunhofer*, 2011. URL http://www.marcuswinter.de/media/other/huygens-construction.png.